

Electrical characteristics of Ni Ohmic contact on n-type GeSn

H. Li, H. H. Cheng, L. C. Lee, C. P. Lee, L. H. Su, and Y. W. Suen

Citation: [Applied Physics Letters](#) **104**, 241904 (2014); doi: 10.1063/1.4883748

View online: <http://dx.doi.org/10.1063/1.4883748>

View Table of Contents: <http://scitation.aip.org/content/aip/journal/apl/104/24?ver=pdfcov>

Published by the [AIP Publishing](#)

Articles you may be interested in

[Correlation between microstructure and temperature dependent electrical behavior of annealed Ti/Al/Ni/Au Ohmic contacts to AlGaIn/GaN heterostructures](#)

Appl. Phys. Lett. **103**, 201604 (2013); 10.1063/1.4828839

[Electrical, microstructural, and thermal stability characteristics of Ta/Ti/Ni/Au contacts to n- GaN](#)

J. Appl. Phys. **95**, 1516 (2004); 10.1063/1.1633660

[Effect of an indium-tin-oxide overlayer on transparent Ni/Au ohmic contact on p -type GaN](#)

Appl. Phys. Lett. **82**, 61 (2003); 10.1063/1.1534630

[Low-resistant and high-transparent Ru/Ni ohmic contact on p-type GaN](#)

Appl. Phys. Lett. **80**, 2937 (2002); 10.1063/1.1474609

[Low-resistance Pt/Ni/Au ohmic contacts to p-type GaN](#)

Appl. Phys. Lett. **74**, 70 (1999); 10.1063/1.123954



Electrical characteristics of Ni Ohmic contact on n-type GeSn

H. Li,¹ H. H. Cheng,^{1,a)} L. C. Lee,² C. P. Lee,² L. H. Su,³ and Y. W. Suen³

¹Center for Condensed Matter Sciences and Graduate Institute of Electronics Engineering, National Taiwan University, Taipei 106, Taiwan

²Center for Nano Science and Technology, National Chiao Tung University, Hsinchu 300, Taiwan

³Department of Physics and Institute of Nano Science, National Chung Hsing University, Taichung 402, Taiwan

(Received 2 May 2014; accepted 4 June 2014; published online 16 June 2014)

We report an investigation of the electrical and material characteristics of Ni on an n-type GeSn film under thermal annealing. The current-voltage traces measured with the transmission line method are linear for a wide range of annealing temperatures. The specific contact resistivity was found to decrease with increasing annealing temperature, followed by an increase as the annealing temperature further increased, with a minimum value at an annealing temperature of 350 °C. The material characteristics at the interface layer were measured by energy-dispersive spectrometer, showing that an atomic ratio of (Ni)/(GeSn) = 1:1 yields the lowest specific contact resistivity.

© 2014 AIP Publishing LLC. [<http://dx.doi.org/10.1063/1.4883748>]

The group IV elements Si and Ge are widely used for various devices. In a recent development, another group IV element, Sn, is employed in the growth of group IV materials. The incorporation of Sn changes the physical properties of the host material such as the energy band.^{1,2} This leads to the demonstration of: (a) optical devices, such as GeSn-based light-emitting diodes with room temperature direct emission,^{3,4} and (b) electrical devices, such as metal-oxide-semiconductor field-effect transistor with carrier mobility higher than conventional Ge devices.^{5,6} For both types of devices, electrical Ohmic contact is required for achieving the highest performance. Also, GeSn alloy has been proposed as an active material for laser diodes.^{7,8} Here, we report an investigation of the current-voltage (I-V) characteristics measured with the transmission line method (TLM) of Ni on n-type GeSn film. The results show that the I-V characteristics are linear for a wide range of annealing temperatures. The contact resistivity was found to decrease with increasing annealing temperature, followed by an increase as the annealing temperature further increased, with a minimum value at 350 °C. This observation is attributed to the material characteristics of the interfacial layer of Ni/n-type GeSn formed during the annealing. The composition of the interfacial layer is probed by X-ray energy-dispersive Spectrometer (EDS), and the result shows that an atomic ratio of Ni/(GeSn) = 1:1 yields the lowest contact resistivity. The present investigation determines the optimized annealing temperature for making an electrical Ohmic contact for this material system, which is required for achieving high-performance devices.

Samples were grown on N-type (001) Si substrates by solid-source molecular beam epitaxy (MBE) at a base pressure of 5×10^{-10} Torr. Si and Ge were deposited by a dual E-gun system, and Sn was evaporated using an effusion cell equipped with dual heating filaments placed at the bottom and the orifice at the top of the crucible. Prior to loading in the growth chamber, Si wafers were cleaned using the

standard cleaning process. To remove the native oxide layer on the surface, *in situ* thermal annealing at 900 °C, under a low Si flux, was employed for duration of 5 min, until a sharp 2×1 reflection high-energy electron diffraction (RHEED) pattern was observed. The sample consists of (a) a 100-nm un-doped Si layer grown at 700 °C, (b) a 100-nm un-doped Si layer grown at a low temperature of 350 °C, (c) a 100-nm un-doped Ge layer grown at 350 °C, follow by an 800 °C annealing, (d) a 100-nm un-doped Ge layer grown at 500 °C, and (e) a 180-nm n-type GeSn layer doped with antimony (Sb) grown at a low temperature of 150 °C. The growth of different layers was controlled using a shutter placed in front of the sources. Layers (c) and (d) serve as Ge virtual substrates (VS) for the subsequent growth of layers (e). The GeSn layer was grown at a temperature below the melting point of Sn to suppress surface segregation.⁹ The doping concentration of the layer was characterized by four-point Hall measurement, and the carrier concentration was found to be $2 \times 10^{18} \text{ cm}^{-3}$. The sample was annealed at temperatures between 250 and 400 °C for 30 s using rapid thermal annealing (RTA). Higher annealing temperatures are not employed, as GeSn layer begins to relax in the film at $T > 400 \text{ °C}$.¹⁰

Different experimental techniques were employed to characterize the samples. High-resolution X-ray diffraction in both (004) ω - 2θ scanning and (224) reciprocal space mapping (RSM) was performed, by which lattice constant in the growth direction (a^{\perp}) and perpendicular to the growth direction (a^{\parallel}) can be calculated.¹⁰ Cross-sectional transmission electron microscopy (XTEM) was conducted to investigate the microstructure of the film. EDS measurements (Model X-Max, Oxford Instrument) with a spot size of 1 nm were performed to determine the presence of different elements at the Ni/n-type GeSn interface. For the electrical measurement, nickel (Ni) was used for the contact, as it has a relatively low resistance among the commonly used transition metals on germanium.¹¹ A layer of 30 nm Ni was deposited using an e-beam evaporator. The TLM was used for the I-V measurement. Five rectangular parallel metal pads were fabricated by standard processing techniques with dimensions

^{a)}Author to whom correspondence should be addressed. Electronic mail: hhcheng@ntu.edu.tw.

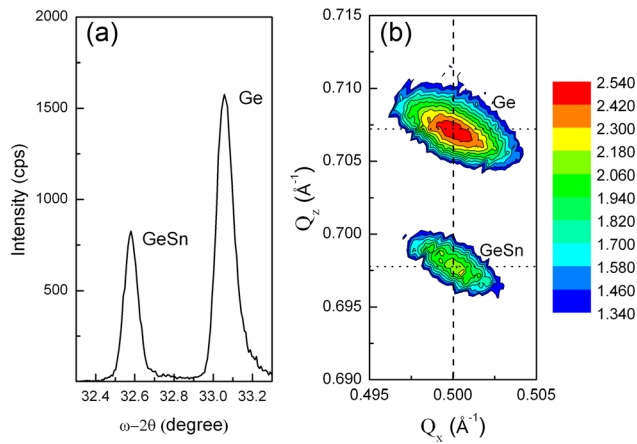


FIG. 1. (a) X-ray (004) ω - 2θ scan and (b) (224) RSM for as-grown sample.

of $2\text{ mm} \times 0.2\text{ mm}$, and the spacing (L) between the metal pads was 0.2, 0.4, 0.6, and 0.8 mm.

First, we present the results of X-ray measurement. The spectra of both the (004) reflection and (224) RSM around the Ge peak of the sample without annealing are plotted in Fig. 1. Two features are clearly resolved, associated with the relaxed Ge buffer layer and the GeSn epilayer. In the (004) scanning as shown in Fig. 1(a), the peak position of GeSn sits at lower angle than the Ge peak owing to a larger lattice constant in growth direction. In the (224) RSM as shown in Fig. 1(b), the position of the GeSn is located at the same Q_x ($\sqrt{8}/a^{\parallel}$) with Ge, as marked by the vertical dashed line. This indicates that the GeSn layer is coherently strained. From an

analysis, a^{\perp} and a^{\parallel} can be found. Knowing these values, the strain of the layer is calculated and the results show that the layer is fully strained. The Sn composition of the layer, in comparison with the composition-dependent lattice constant of GeSn alloy, is found to be 4.9%. Upon annealing below $400\text{ }^{\circ}\text{C}$, the peak position of the GeSn remains unchanged for all samples; therefore, the strain and composition of the GeSn layer are unaffected by the thermal process. We would like to point out that, although the two physical characteristics of the GeSn layer remain unchanged for all samples, the defect density is different. As estimated from the full width at half maximum (FWHM) of rocking curve,¹² the defect density increases with increasing annealing temperatures from $1 \times 10^8\text{ cm}^{-2}$ to $1.4 \times 10^8\text{ cm}^{-2}$.

Next, we consider the microstructure of the film. For the as-grown sample, threading dislocations are not observed in the GeSn layer but trapped in the Ge VS. In the case where annealing is done, dislocations are also not seen; the typical XTEM image (for a sample annealed at $400\text{ }^{\circ}\text{C}$) is depicted in Figure 2(a). With annealing, however, a thin layer is observed at the Ni/GeSn interface, as marked by the dotted circle. The thickness of this interfacial layer is $\sim 4\text{ nm}$, as measured by the high-resolution XTEM, as plotted in Figure 2(b). This layer is formed during the thermal annealing and is attributed to the alloying effect.

The I-V trace of the sample annealed at $350\text{ }^{\circ}\text{C}$ is plotted in Fig. 3(a). It shows a linear dependence on gap spacing which is the characteristic of Ohmic contact. The resistance

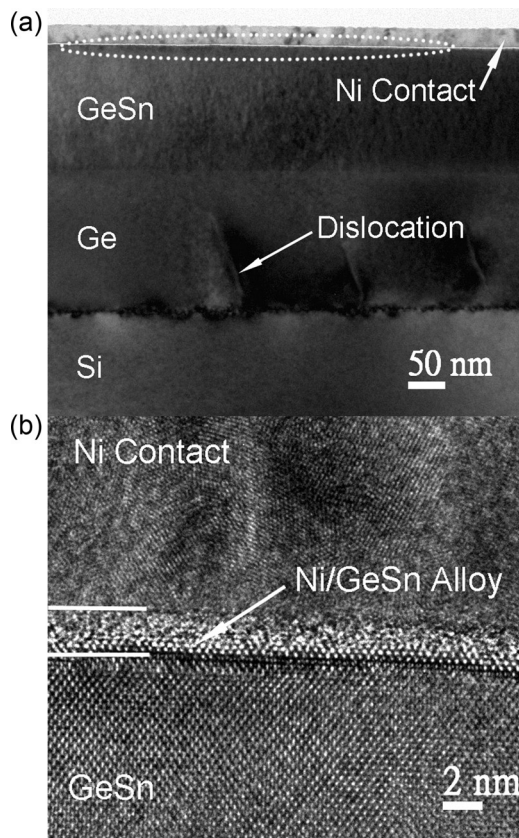


FIG. 2. (a) XTEM image of sample annealed at $350\text{ }^{\circ}\text{C}$. (b) High resolution image taken at the Ni/GeSn interface.

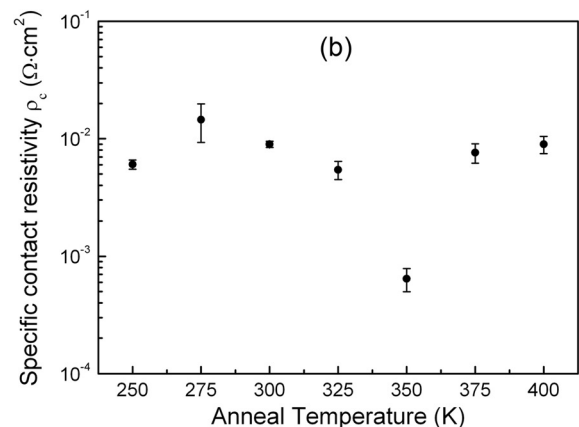
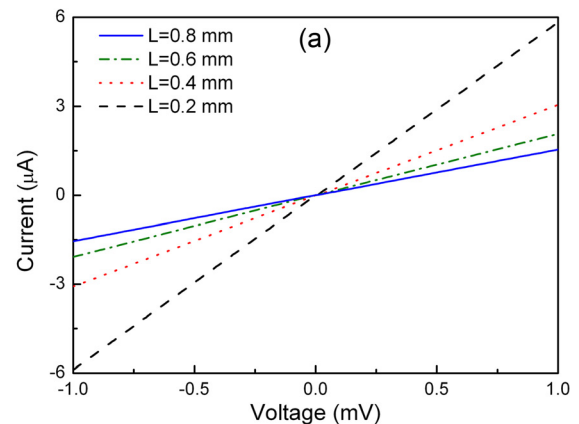


FIG. 3. (a) A family of I - V curves with the different gap spacings for samples annealed at $350\text{ }^{\circ}\text{C}$. (b) Specific contact resistivity of the samples annealed at different temperatures.

increases linearly with increasing contact spacing, which can be attributed to the increase in the bulk resistance. Similar linear behavior is also observed for the other samples, but with different resistances. The measured resistance (R_m) is a sum of the intrinsic bulk resistance (R_b) and contact resistance (R_C). ($R_m = R_b + 2R_C$). In terms of sheet resistance (R_S), to a good approximation, the measured resistance can be written as follows:¹³

$$R_m = \frac{R_S}{W}L + 2\frac{R_S L_T}{W},$$

where W is the width of the metallic contact and $L_T = \sqrt{\rho_C/R_S}$ is the transfer length. ρ_C is the specific contact resistivity, which, to a good approximation, $\approx R_C L_T W$. Using the physical parameters of the metal contact described above and the measured R_m with different gap spacings, ρ_C can be found. The specific contact resistivity for samples annealed at different temperatures is plotted in Figure 3(b). It shows that ρ_C decreases with increasing annealing temperature, reaching a minimum of $6.4 \pm 1.5 \times 10^{-4} \Omega\text{-cm}^2$ at 350 °C, followed by an increase with further increases in temperature.

In the electrical characteristic described above, the I-V traces are linear for all samples, but with different resistances. The difference is caused by the material characteristics of the interfacial layer. EDS measurements were performed at ten various locations to probe the composition of the interfacial layer. Taking the average value from these measured points, the results are categorized into two regions: (a) for samples annealed below 350 °C, the atomic ratio of Ni/(Ge_{0.955}Sn_{0.045}) is larger than 1 (for example, the sample annealed at 300 °C, the ratio is ~ 1.55), while (b) the atomic ratio is close to 1:1 for samples annealed at or above 350 °C. This revealed that, the Ni mono-stannogermanide phase of the interfacial layer gives the lowest ρ_C .¹⁴ With increasing annealing temperatures, although the material characteristics of the interfacial layer remain unchanged, nevertheless, ρ_C becomes larger. This is attributed to the increase of defect density in the GeSn layer, which leads to degradation of the crystal quality of the interfacial layer, resulting in an increase in the specific contact resistivity.

In summary, the electrical characteristics of contact resistivity and the material characteristics of Ni on n-type GeSn were investigated. By analyzing the I-V curve measured with the transmission line method, ρ_C is found to be the lowest for samples annealed at 350 °C associated with the material characteristics of the interfacial layer formed during annealing. In establishing the optimized specific contact resistivity, we would like to point out that, as ρ_C is inversely proportional to the Schottky barrier width,¹⁵ we expect that the value could be reduced by increasing the doping level in the GeSn layer.

The authors would like to thank the National Science Council of the Republic of China for its financial support under Grant No. 101-2112-M-002-015-MY3, and the U.S. Air Force Office of Scientific Research under Grant No. FA2386-11-1-4113 (Program Managers Dr. Jermont Chen and Dr. Gernot Pomrenke).

- ¹R. Chen, H. Lin, Y. Huo, C. Hitzman, T. I. Kamins, and J. S. Harris, *Appl. Phys. Lett.* **99**, 181125 (2011).
- ²J. Mathews, R. T. Beeler, J. Tolle, C. Xu, R. Roucka, J. Kouvetakis, and J. Menéndez, *Appl. Phys. Lett.* **97**, 221912 (2010).
- ³H. H. Tseng, K. Y. Wu, H. Li, V. Mashanov, H. H. Cheng, G. Sun, and R. A. Soref, *Appl. Phys. Lett.* **102**, 182106 (2013).
- ⁴M. Oehme, K. Kostecki, T. Arguirov, G. Mussler, K. Ye, M. Gollhofer, M. Schmid, M. Kaschel, R. Körner, M. Kittler, D. Buca, E. Kasper, and J. Schulze, *IEEE Photonics Technol. Lett.* **26**, 187 (2014).
- ⁵G. Han, S. Su, C. Zhan, Y. Yang, L. Wang, P. Guo, W. Wei, C. P. Wong, Z. X. Shen, B. Cheng, and Y.-C. Yeo, *IEEE Int. Electron Devices Meet.* **2011**, 402.
- ⁶J. D. Sau and M. L. Cohen, *Phys. Rev. B* **75**, 045208 (2007).
- ⁷G. Sun, R. A. Soref, and H. H. Cheng, *J. Appl. Phys.* **108**, 033107 (2010).
- ⁸G. Sun, R. A. Soref, and H. H. Cheng, *Opt. Express* **18**, 19957–19965 (2010).
- ⁹E. Kasper, J. Werner, M. Oehme, S. Escoubas, N. Burle, and J. Schulze, *Thin Solid Films* **520**, 3195 (2012).
- ¹⁰H. Li, Y. X. Cui, K. Y. Wu, W. K. Tseng, H. H. Cheng, and H. Chen, *Appl. Phys. Lett.* **102**, 251907 (2013).
- ¹¹S. Gaudet, C. Detavernier, A. J. Kellock, P. Desjardins, and C. Lavoie, *J. Vac. Sci. Technol., A* **24**, 474 (2006).
- ¹²J. E. Ayers, *J. Cryst. Growth* **135**, 71 (1994).
- ¹³D. K. Schroder, *Semiconductor Material and Device Characterisation*, 3rd ed. (John Wiley & Sons, Hoboken, New Jersey, 2006).
- ¹⁴Y. Liu, H. Wang, J. Yan, and G. Han, *ECS Solid State Lett.* **3**, P11 (2014).
- ¹⁵A. Firrincieli, K. Martens, E. Simoen, C. Claeys, and J. A. Kittl, *Microelectron. Eng.* **106**, 129 (2013).